J Solid State Electrochem (2008) 12:113–119
DOI 10.1007/s10008-007-0368-3

ORIGINAL PAPER

Oxygen reduction reaction on (Pt–$NbPO_x$)/MWCNTs electrodes prepared by microwave irradiation method

Jian-Shu Huang · Xiao-Gang Zhang · Jian-Min Luo · Jing-Yu Sun · Wen-Jian Yang

Received: 30 October 2006 / Revised: 27 March 2007 / Accepted: 23 May 2007 / Published online: 7 July 2007

Abstract (Pt–$NbPO_x$)/multi-walled carbon nanotubes (MWCNTs) with different $NbPO_x$ MWCNTs were prepared by a simple microwave irradiation method. The (Pt–$NbPO_x$)/MWCNTs catalyst was characterized, and the kinetics toward oxygen reduction reaction (ORR) was determined, compared with that of Pt/MWCNTs catalyst. It was found that 10 wt% $NbPO_x$ was the best loading in terms of current density. The number of exchange electrons for the ORR was found to be close to four on both (Pt–$NbPO_x$)/MWCNTs and Pt/MWCNTs.

Keywords Electrocatalyst · $NbPO_x$ · MWCNTs · Oxygen reduction reaction (ORR)

Introduction

A major impediment to the commercialization of fuel cell technology is the low activity of platinum electrocatalyst used for oxygen reduction [1–3]. Platinum has been alloyed with transition metals like Ni, Co, etc, which show higher activity than that of pure Pt [4, 5]. However, Pt is an expensive metal of low abundance, and hence, finding a non-noble-metal alternative is of interest. Zhang et al. [6] studied the ORR of nano-manganese oxide and cobalt octacyanophthalocyanine in alkaline media. Other materials like oxides [7], nitrides [8, 9], oxynitride [10], macrocycle [11–13], and carbide [14] have been investigated as electrocatalysts for the ORR and their stability in alkaline and acid media.

The mechanism and kinetics of the oxygen reduction reaction (ORR) greatly depend on the choice of active materials. The composition structure and nature of the active substrate material are key to successful development of new electrode for ORR. Carbon nanotubes (CNTs), as a new form of carbon, have been suggested to be suitable catalyst supports [15, 16] for air electrode due to their highly accessible surface area, low resistance, and high stability. In our previous works [17–19], different forms of carbon as catalyst supports were successfully prepared and characterized. These composite materials have shown good catalytic activity and high catalytic oxygen reduction efficiency compared with the other common active materials. Recently, it was reported that the catalytic activity of platinum-based electrocatalyst was enhanced when it was dispersed on iron phosphate [20, 21]. Hydrous transition metal phosphates are good proton and water conductors. Phosphate can also be less prone to poisoning (electrochemical activity degradation) than that of metals. Phosphates are also known for their oxygen affinity and therefore should increase the amount of oxygen transport and store at the cathode. Many phosphate catalysts are resistant to dissolving under the highly corrosive condition and not limited to iron, niobium, tin, tungsten, molybdenum, antimony, vanadium, tantalum, chromium, zinc, titanium, zirconium, and cobalt. The phosphate catalyst can also be combined with another conductive support, which can provide additional electron conduction and reduce the amount of phosphate catalyst needed [22]. In this paper, platinum–niobium phosphate on multi-walled carbon nanotubes (MWCNTs) support [(Pt-NbPOx)/MWCNTs] was prepared by microwave irradiation method, and then its electrocatalytic activity toward ORR was investigated by the rotating disk

J.-S. Huang · J.-M. Luo · J.-Y. Sun · W.-J. Yang
Institute of Applied Chemistry, Xinjiang University, Urumqi 830046, People's Republic of China

X.-G. Zhang (✉)
College of Material Science and Engineering, Nanjing University of Aeronautics and Astronautics, Nanjing 210016, People's Republic of China
e-mail: azhangxg@nuaa.edu.cn

electrode (RDE) technique, which is a powerful tool for the kinetics of ORR [23, 24]. The kinetic rate constants of ORR were evaluated through a Koutecky–Levich plot and Levich equation. The number of exchange electrons for ORR is found to be close to four.

Experimental section

Oxidation treatment for MWCNTs

MWCNTs were purchased from Shenzhen Nanotech Port (Shenzhen, China) and purified to >95%. The MWCNTs had an outer diameter of 20–40 nm. The acid solution was used for the oxidation treatment of MWCNTs following the procedure [15]. Briefly, 1.0 g of MWCNTs was dispersed in 150 ml HNO_3 (65%) solution under vigorous stirring and refluxed at 393 K for 10 h. The resulting MWCNTs was rinsed thoroughly to neutral with deionized water and then dried at 373 K for 24 h.

Loading of nanoparticle catalysts on CNTs

Varying amounts of $NbCl_5$ (98%, from ACROS) were dissolved in 150 ml ethanol. The pre-treated MWCNTs was added and impregnated with $NbCl_5$ stirring at room temperature for 12 h, and then ultrasonic treatment for 0.5 h. Fifteen milliliters 10% H_3PO_4 was dropped into the solution under vigorous stirring [22]. Two milliliters hexachloroplatinic acid ($H_2PtCl_6{\cdot}6H_2O$) (7.5 mg Pt/ml) ethanol solution was added into the mixed solution, and pH was adjusted up to 10 by 0.5 mol l^{-1} $NH_3{\cdot}H_2O$. Ethylene glycol (EG) of 7.5 ml was dropped into the solution. The mixture was heated in a household microwave oven (China, 2,450 MHz, at a fixed power level of 500 W) for 50 s. The resulting suspension was filtered, and the residue was washed with acetone and then dried at 373 K for 12 h in a vacuum oven [25]. Pt was 10 wt% and $NbPO_x$ was 5, 10, 15% by weight based on the final (Pt–$NbPO_x$)/MWCNTs catalyst, and marked as A, B, and C, respectively. As comparison, 10 wt% Pt/MWCNTs was obtained by the similar microwave irradiation reduction procedure, marked as D.

Preparation of electrode

A RDE with glassy carbon (GC; 3 mm diameter) was pretreated and used as working electrode [26]. (Pt-$NbPO_x$)/MWCNTs and Pt/MWCNTs were dispersed in 0.05% Nafion (Aldrich) solution, and the resultant suspension was agitated in an ultrasonic bath for 30 min. (Pt-$NbPO_x$)/MWCNTs/Nafion- or Pt/MWCNTs/Nafion-modified electrodes were obtained by a drop of suspension coated on the surface of GC electrode then air-dried for 1 h.

Instruments and measurement

The morphology of the catalysts was investigated by scanning electron microscope (SEM; Leo1430VP) and transmission electron microscope (TEM; Hitachi H-600). Energy dispersion spectrum (EDS) analysis (Leo1430VP SEM) was used to characterize the chemical composition of the catalyst. The RDE was used as working electrode, Ag/AgCl (saturated with KCl) as reference electrode, and platinum wire as an auxiliary electrode, respectively. Electrochemical measurements were performed with an Autolab PGSTAT302 (Metrohm, Switzerland) electrochem-

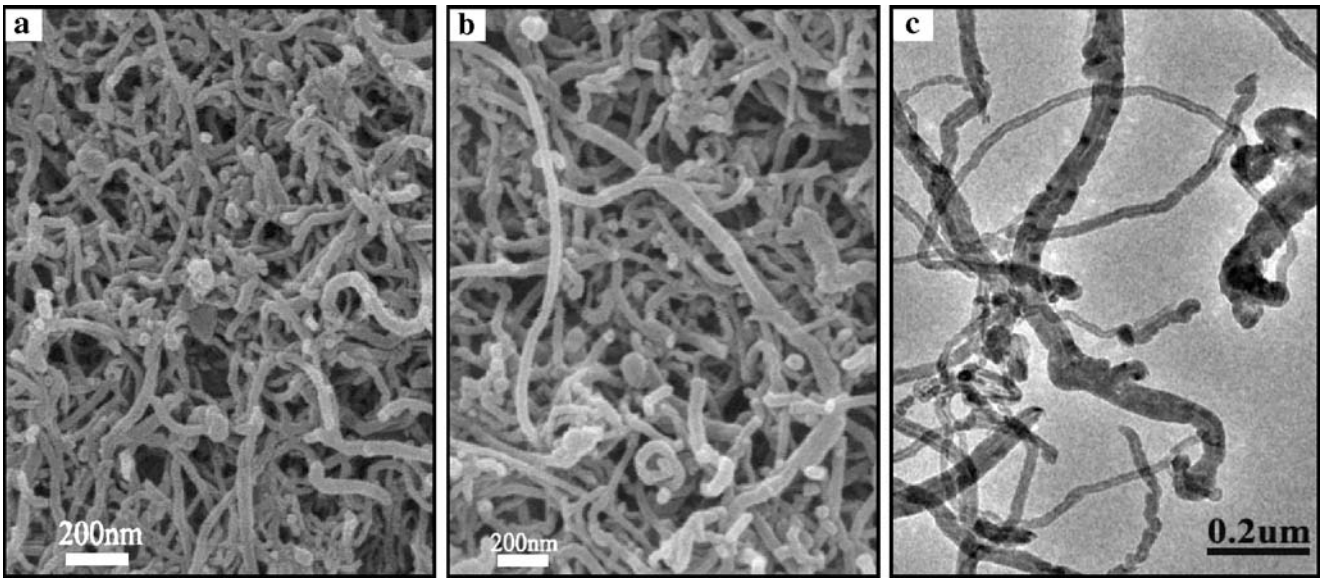

Fig. 1 SEM images of catalyst B (**a**) D (**b**) and TEM image of B (**c**)

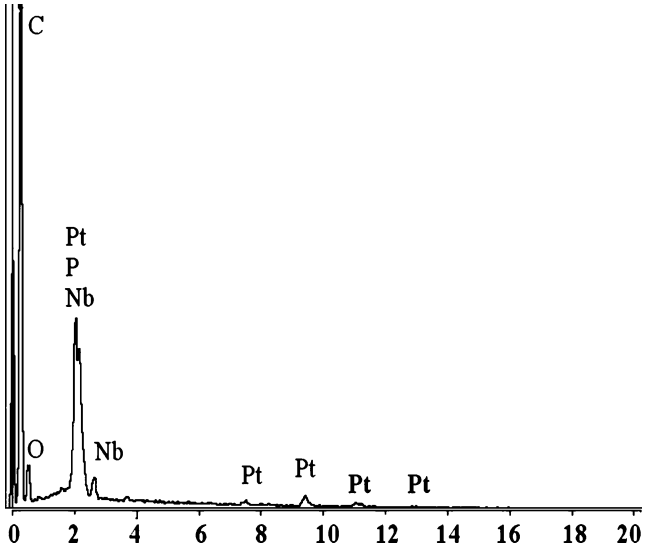

Fig. 2 Energy dispersion spectrum analysis of catalyst B

ical workstation in the potential range of 0~−1.2 V. The rotation rates were controlled by Model 636 motor controller (EG&G, USA). All electrochemical experiments were performed in 1 mol L^{-1} KOH aqueous solution saturated with O_2 at 298 K.

Result and discussion

Analysis of morphology and composition

The SEM images of the as-prepared B (Fig. 1a) catalyst and D (Fig. 1b) are shown in Fig. 1. It can be seen that catalyst is dispersed on the surface of MWCNTs. Although particle size could also play a significant role in the catalytic activity [27], significant variations in particle size with catalyst content are not observed.

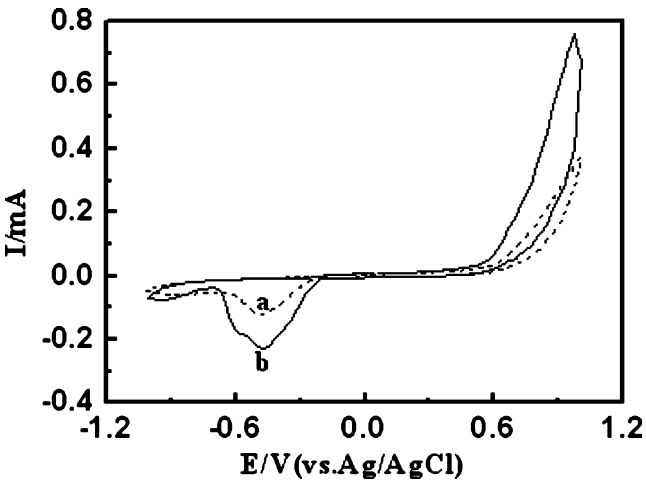

Fig. 3 Cyclic voltammograms at D/Nafion-modified (*a*) and B/Nafion- (*b*) glass carbon (GC) electrodes in O_2 saturated 1 mol l^{-1} KOH solution. Scan rate: 5 mVs^{-1}

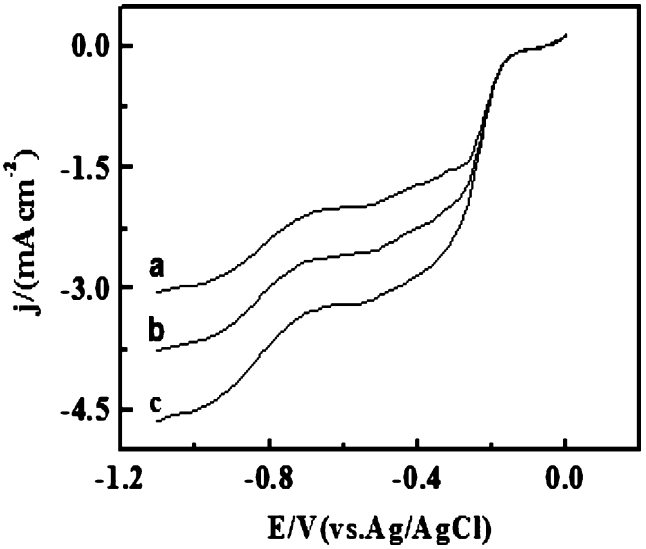

Fig. 4 $j(E)$ curves at a rotation rate ω=1,600 rpm recorded in O_2 saturated 1 mol l^{-1} KOH solution for: C (*a*), A (*b*), and B (*c*). Scan rate: 5 mV s^{-1}

TEM image of B catalyst (Fig. 1c) shows the dispersion of particles on the MWCNTs surface. The result demonstrates that nanoparticles have evidently formed on the MWCNTs support by microwave-assisted heating of H_2PtCl_6 in EG solution. The size of metal nanoparticles is determined by the reduction rate of the metal precursor. The dielectric constant (41.4 at 298 K) of EG are high, thus rapid heating occurs easily under microwave irradiation. In EG-mediated reactions (the 'polyol' process), EG also acts as the reductive agent. The fast heating by microwave accelerates the reduction of metal precursor and the nucleation of metal clusters. The ease of the nucleation-limited process greatly assists in small particle formation.

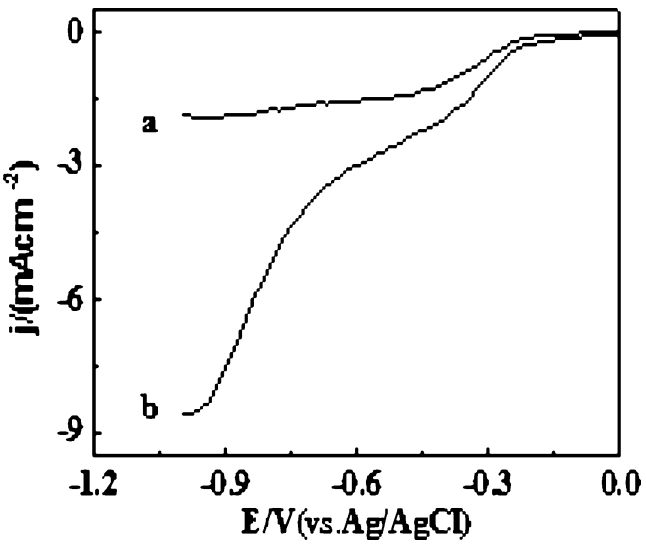

Fig. 5 $j(E)$ curves at a rotation rate ω=1600 rpm recorded in O_2 saturated 1 mol l^{-1} KOH solution for: D (*a*) and B (*b*). Scan rate: 5 mV s^{-1}

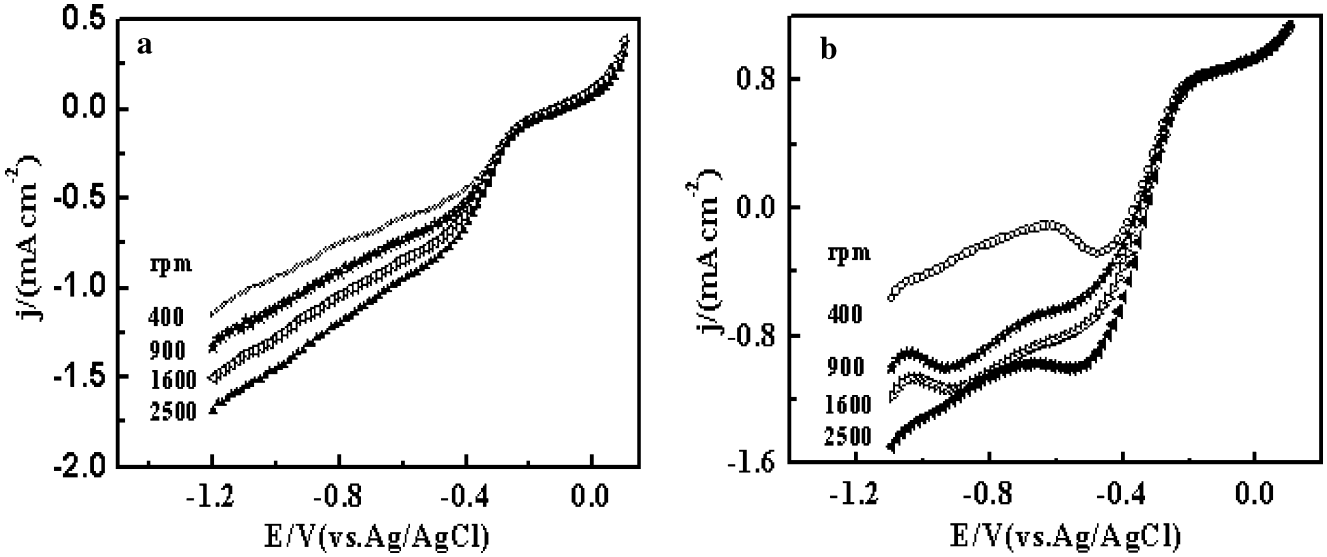

Fig. 6 $j(E)$ curves at different rotation rate Ω recorded in O_2 saturated 1 mol l^{-1} KOH solution for: B (**a**) and D (**b**). Scan rate: 5 mV s^{-1} rotation rate was indicated in the graph

Additionally, the homogeneous microwave heating reduces the gradients of temperature and concentration in the reaction medium and provides a more uniform environment for the nucleation and growth of metal particles. The carbon surface has the suitable sites for heterogeneous nucleation and interrupts particle growth [25].

To investigate the composition of the (Pt–$NbPO_x$)/MWCNTs catalyst, EDS analysis was carried out. The EDS spectrum of B catalyst clearly shows the presence of Pt, Nb, P, and O elements in the final product (depicted in Fig. 2).

Cyclic voltammetry study

The electrocatalytic properties of B and D for ORR are shown in Fig. 3. The (Pt–$NbPO_x$)/MWCNTs/Nafion- or Pt/MWCNTs/Nafion-modified GC electrodes exhibits a well-defined reduction peak approximately at −0.4 V in O_2 saturated KOH solution. In summary, the obvious enhancement of the cathodic current for (Pt–$NbPO_x$)/MWCNTs electrode indicates that the electrocatalytic activity of B is higher than that of D for ORR.

Electrocatalytic activity towards ORR

Figure 4 presents the $j(E)$ polarization curves for (Pt–$NbPO_x$)/MWCNTs/Nafion with a loading 5, 10, and 15 wt% $NbPO_x$ at a rotation rate of 1,600 rpm. The higher current densities were obtained.

The polarization curves of the oxygen reduction in the 1 mol l^{-1} KOH solution at room temperature were detected

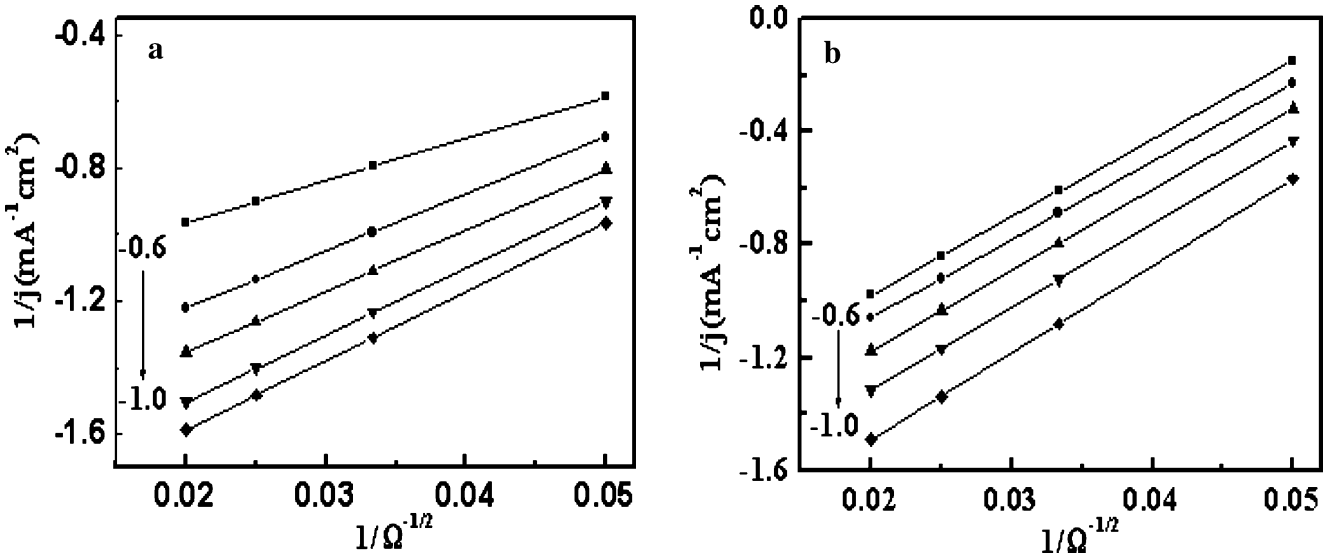

Fig. 7 Koutecky–Levich plots for catalyst B (**a**) and D (**b**) catalysts at different potentials: −0.6, −0.7, −0.8, −0.9, −1.0 V vs Ag/AgCl

Table 1 Kinetic parameters for catalytic reduction of oxygen at B/Nafion- and D/Nafion-modified glass carbon (GC) electrodes in O_2 saturated 1 mol L^{-1} KOH solution

E/V vs Ag/AgCl	(Pt–$NbPO_x$/MWCNTs			Pt/MWCNTs		
	K–L slopes	n(mol)	$K\Gamma_{cat}$(cm/s)	*K–L* slopes	n(mol)	$K\Gamma_{cat}$(cm/s)s
−1.0	9.75	3.85	0.072	10.82	3.50	0.041
−0.9	9.85	3.71	0.086	10.65	3.46	0.053
−0.8	9.71	3.87	0.065	10.94	3.49	0.038
−0.7	9.86	3.69	0.073	10.71	3.52	0.027
−0.6	9.56	3.87	0.081	10.48	3.59	0.044

between 0 to −1.2 V and characterized of (Pt–$NbPO_x$)/MWCNTs and Pt/MWCNTs electrocatalyst in this solution. The larger cathodic current indicates that a higher electrocatalytic activity is obtained with 10 wt% $NbPO_x$ loading. Excessive phosphate is thought to decrease the active area of the MWCNTs accessible to hydrogen peroxide and thus leads to a partial loss of its catalytic disproportionation activity towards hydrogen peroxide. In the low current density region, the voltage drop in the potential–current curve, generally known as activation polarization, reflects the sluggish kinetics intrinsic to the ORR at the cathode surface.

As shown in Fig. 5, the onset of reduction wave at B catalyst shifted towards positive potential for about 50 mV in comparison with that of D catalyst. The current density of B/Nafion-modified electrode is larger than that of D/Nafion-modified at equal rotation rates. This indicates that (Pt–$NbPO_x$)/MWCNTs has better electrocatalytic activity than that of Pt/MWCNTs.

Kinetic of oxygen reduction

Figure 6 shows the polarization curves of ORR obtained at different rotation rates for B (Fig. 6a) and D (Fig. 6b) catalyst in 1 mol l^{-1} KOH solution. The Koutecky–Levich plots $1/j$ vs $1/\omega^{-1/2}$ are shown in Fig. 7.

According to the Levich and Koutecky–Levich equations [28]

$$i_L = 0.620nFAD_0^{2/3}\omega^{1/2}\nu^{-1/6}C_0^* \quad (1)$$

$$i_K = nFAK\Gamma_{cat}C_0^* \quad (2)$$

$$i^{-1} = i_K^{-1} + i_L^{-1} \quad (3)$$

$$i^{-1} = 1/\left(nFAK\Gamma_{cat}C_0^*\right) + 1/\left(0.620nFAD_0^{2/3}\omega^{1/2}\nu^{-1/6}C_0^*\right) \quad (4)$$

where i_L (A) is the limiting current for the electrode reaction of reactive species by the diffusion-controlled process, i_K (A) is the kinetic current for the reaction of reactive species at the electrode surface, n (mol^{-1}) is the electron transfer number per mole of reactive species, F (96,500 C mol^{-1}) is Faraday constant, A (cm^2) is the electrode area, D_0 (cm^2 s^{-1}) is the diffusion coefficient of O_2 in 1 mol l^{-1} KOH solution

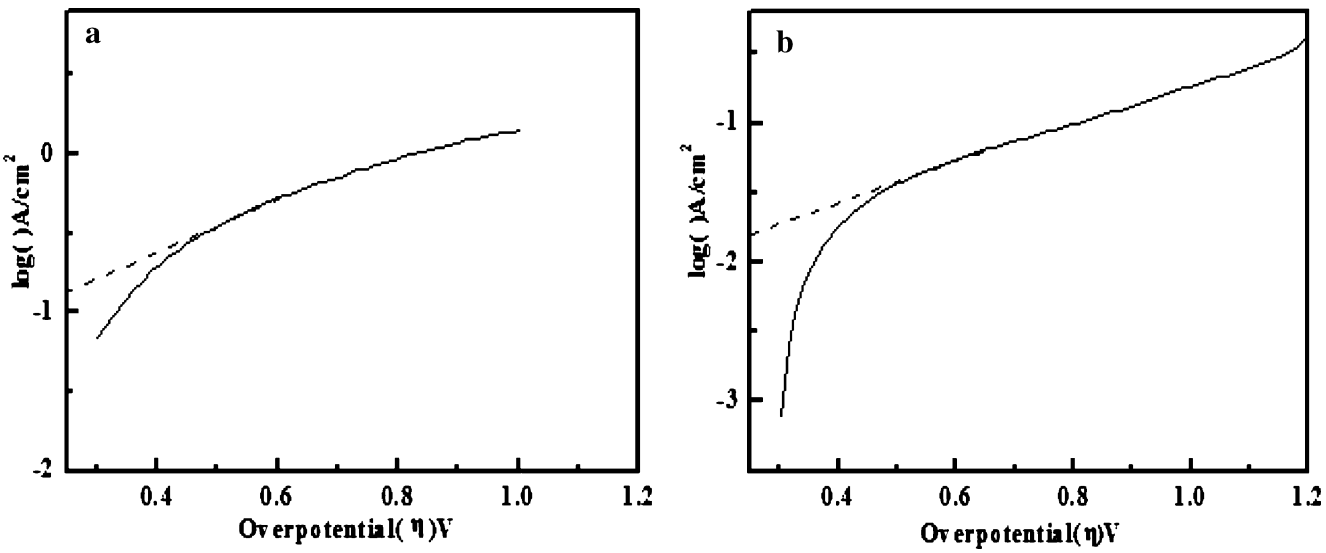

Fig. 8 Tafel polarization curves of B/Nafion- (**a**) and D/Nafion-modified glass carbon (GC) electrodes (**b**)

(=1.76×10^{-5} cm^2 s^{-1}), $\omega(s^{-1})$ is rotation rate, $\nu(cm^2\ s^{-1})$ is kinetic viscosity of solution (=0.01 cm^2 s^{-1}), C_0^* (mol cm^{-3}) is the concentration of O_2 in 1 mol l^{-1} KOH solution at 298 K (=1.103×10^{-6} mol cm^{-3}) [29], K (M^{-1} s^{-1}) is kinetic rate constant for catalytic reaction, and Γ_{cat} (mol cm^{-2}) is the quantity of catalyst on the surface of the electrode. The kinetic analysis result of ORR at the modified electrode was summarized in Table 1.

Those reactions at B/Nafion- and D/Nafion-modified electrode were an approximately direct four-electron process. With the decrease of potential, the rate constant becomes significantly larger and the kinetic rate constant for catalytic reaction is also of the same order. The analysis shows that (Pt–$NbPO_x$)/MWCNTs electrode has the higher electrocatalytic activity for ORR, and $NbPO_x$ could enhance the utilization of Pt. MPO_x (M=metal) has microporous open frame work structure, which can facilitate high protonic conduction [30]. This suggested that the activity of (Pt–$NbPO_x$)/MWCNTs was improved due to both $NbPO_x$ and MWCNTs, which enhanced the contact area of three phases. It is well known that the ORR is a complex process including many electrochemical (chemical) steps with different intermediates [31]. Toda et al. [32] and Mukerjee et al. [33] explained that the improvement to the catalytic activity was based on an increase of the d-orbital vacancy, promoting a stronger metal–oxygen (M–O) interaction and the formation of stronger $Pt-O_2^-$ bond with the adsorbed O_2^- species. The stronger $Pt-O_2^-$ bond can cause a weakening and lengthening of the O–O bond and an easier scission of the O–O bond, resulting in an increase in the reaction rate. Shukla et al. [34] and Arico et al. [35], on the other hand, have attributed the increased catalytic activity to a decrease in surface oxides and an enrichment of active Pt sites. Mukerjee et al. [33] explained the enhancement in activity based on the decrease in the Pt–Pt distance and the Pt–Pt coordination numbers. Better catalytic efficiency for oxygen reduction is caused by facilitation of O_2 interactions with the adsorption sites (so-called active sites) on the surface of the catalyst [36, 37].

Tafel measurements

A plot of log i vs overpotential (η) for the B/Nafion-(a) and D/Nafion-(b) modified electrodes was shown in Fig. 8. The Tafel slope is −70 mV/decades for the (Pt–$NbPO_x$)/MWCNTs/Nafion-electrode and −100 mV/decade for the Pt/MWCNTs/Nafion-electrode. Any correction has not been used for any mass transfer effects, and the values vary depending upon the substrates [38]. The slope observed for the Pt/MWCNTs/Nafion-electrode is consistent with literature values [39, 40]. The exchange current density is obtained by extrapolating the linear region to zero overpotential. The value of exchange current density obtained from this analysis is 1.2×10^{-4}A cm^{-2} for (Pt–$NbPO_x$)/MWCNTs/Nafion, which is an order of magnified higher than the value of 1.8×10^{-5}A cm^{-2} for the Pt/MWCNTs/Nafion-electrode. The former value compares very favorably with the value of 1.09×10^{-7}A cm^{-2} reported for a commercial catalyst such as Platinum black [41]. Because the exchanged current density depends on the nature of the electrode [42], this suggests that the (Pt–$NbPO_x$)/MWCNTs is a better electrocatalyst to promote the ORR.

Conclusion

(Pt–$NbPO_x$)/MWCNTs catalyst has been prepared by microwave irradiation reduction method. Compared to Pt/MWCNTs, (Pt–$NbPO_x$)/MWCNTs shows better electrocatalytic activity towards ORR in KOH solution. (Pt–$NbPO_x$)/MWCNTs catalyst with initial 10 wt% $NbPO_x$ shows the best performance. MWCNTs as the support should be emphasized in terms of increase of the catalyst active surface, the coordination effect of catalyst, and the distribution of active catalytic sites.

Acknowledgment This work was supported by the National Natural Science Foundation of China (No. 20403014, No.20633040) and National Natural Science Foundation of Jiangsu Province (No. BK2006196).

References

1. Brandon NP, Skinner S, Steele BCH (2003) Ann Rev Mater Res 33:183
2. Benitez R, Chaparro AM, Daza L (2005) J Power Sources 151:2
3. Soderberg JN, Sirk AHC, Campbell SA, Birss VI (2005) J Electrochem Soc 152:A2017
4. He T, Kreidler E, Xiong L, Luo J, Zhong CJ (2006) J Electrochem Soc 153:A1637
5. Baker WS, Pietron JJ, Teliska ME, Bouwman PJ, Ramaker DE, Swider-Lyons KE (2006) J Electrochem Soc 153:A1702
6. Zhang D, Chi DH, Okajima T, Ohsaka T (2007) Electrochim Acta 52:5400
7. Kim JH, Ishihara A, Mitsushima S, Kamiya N, Ota KI (2007) Electrochim Acta 52:2492
8. Jaouen F, Dodelet JP (2007) Electrochim Acta 52:5975
9. Zhong HX, Zhang HM, Liu G, Liang YM, Hu JW, Yi BL (2006) Electrochem Commun 8(5):707
10. Chojak M, Kolary-Zurowska A, Wlodarczyk R, Miecznikowski K, Karnicka K, Palys B, Marassi R, Kulesza PJ (2007) Electrochim Acta 52:5574
11. Li XG, Hsing IM (2007) Electrochim Acta 52:5462
12. Liu HS, Song CJ, Tang YH, Zhang JL, Zhang JJ (2007) Electrochim Acta 52:4532
13. Kullapere M, Tammeveski K (2007) Electrochem Commun 9:1196
14. Nie M, Shen PK, Wei ZD (2007) J Power Sources 167:69
15. Yu RQ, Chen LW, Liu QP, Lin JY, Tan KL, Ng SC (1998) Chem Mater 10:718

16. Tang H, Chen JH, Huang ZP, Wang DZ, Ren ZF, Nie LH (2004) Carbon 24:191
17. Zhang GQ, Zhang XG (2004) Electrochim Acta 49:873
18. Zhang GQ, Zhang XG, Wang YG (2004) Carbon 42:3097
19. Hu FP, Zhang XG, Xiao F, Zhang JL (2005) Carbon 43:2931
20. Bouwman PJ, Dmowski W, Stanley J, Cotton GB, Swider-Lyons KE (2004) J Electroanl Soc 151:A1989
21. Bose AB, Sarkar M, Ro RN (2006) J Power Sources 157:188
22. Lyons KS, Alexandria, Bouwan PJ, Cronfto (2005) US Patent 0,069,753
23. Jin YD, Shen Y, Dong SJ (2004) J Phys Chem B 108:8142
24. Li QW, Yan H, Cheng Y, Zhang J, Liu ZF (2002) J Mater Chem 2:179
25. Liu ZL, Gan LM, Hong L, Chen WX, Lee JY (2005) J Power Sources 139:73
26. Ohsaka T, Mao L, Arihara K, Sotomura T (2004) Electrochem Commun 6:273
27. Shim J, Yoo DY, Lee JS (2000) Electrochim Acta 45:1943
28. Jiang RZ, Chu D (2000) Electrochim Acta 45:4025
29. Jiang RZ, Anson FC (1991) J Electroanal Chem 305:171
30. Cheetham AK, Ferey G, Loiseau T (1999) Angew Chem Int Ed 38:3268
31. Zhang L, Zhang JJ, David P, Wilkinson, Wang HJ (2006) J Power Sources 156:177
32. Toda T, Igarashi H, Watanabe M (1999) J Electroanal Chem 460:258
33. Mukerjee S, Srinivasan S, Soriaga MP, Breen JM (1995) J Phys Chem 99:4577
34. Shukla AK, Neergat M, Bera P, Jayaram V, Hegde MS (2001) J Electroanal Chem 504:111
35. Arico AS, Shukla AK, Kim H, Park S, Min M, Antonucci V (2001) Appl Surf Sci 172:33
36. Xiong L, Kannan AM, Manthiram A (2002) Electrochem Commun 4:898
37. Vracar LM, Krstajic NV, Radmilovic VR, Jaksic MM (2006) J Electroanal Chem 587:99
38. Gojkovic SL, Zecevic SK, Savinell RF (1998) J Electrochem Soc 145:3713
39. Wang J, Swain GM (2003) J Electrochem Soc 150:E24
40. Kita H, Gao YZ, Nakato T, Hattori H (1994) J Electroanal Chem 373:177
41. Britto PJ, Santhanam KSV, Rubio A, Alonso JA, Ajayan PM (1999) Adv Mater 11:154
42. Girishkumar G, Vinodgopal K, Kamat PV (2004) J Phys Chem B 108:19960